Diffraction theory of optimized low-resolution Fresnel encoded lenses

E. Carcolé, J. Campos, I. Juvells, and J. R. de F. Moneo

A mathematical model describing the behavior of low-resolution Fresnel encoded lenses (LRFEL's) encoded in any low-resolution device (e.g., a spatial light modulator) has recently been developed. From this model, an LRFEL with a short focal length was optimized by our imposing the maximum intensity of light onto the optical axis. With this model, analytical expressions for the light-amplitude distribution, the diffraction efficiency, and the frequency response of the optimized LRFEL's are derived.

Key words: Fresnel lens, zone plate, diffraction, spatial light modulator.

1. Introduction

The codification of lenses of variable focal length in optical setups is an important application of pixelated spatial light modulators.[1] The pixelated SLM is a kind of low-resolution device that gives rise to several unwanted effects if a quadratic wave is encoded. These effects and their consequences on lens performance have recently been described in terms of a mathematical theory developed by Carcolé *et al.*[2] Application of this theory permits the light-amplitude distribution at all focal regions to be analytically derived in the Fresnel approximation. The resultant expressions are functions of several nondimensional parameters that are dependent on the characteristics of the low-resolution device and on the encoded focal length. The latter dependence implies a dependence of the amplitude-distribution shape on the focal length. Some important characteristics of these lenses have been studied experimentally.[3]

The main problem with the use of a low-resolution Fresnel encoded lens (LRFEL) as a single lens is its multifocusing property, which gives rise to an important loss of image quality and of diffraction efficiency. An optimization method for the LRFEL has been proposed in Ref. 2. This method is based on the fact that the diffraction pattern of each pixel in the focal plane is just a spherical wave modulated by a sinc function. The sinc function has periodical changes of sign. This implies that certain groups of pixels (named blocks) interfere with opposite sign in the focal region, thereby making the total contribution lower than the maximum available. If we assume that the lens must take the maximum value at the optical axis, the solution to this problem consists of our shifting in π the phases of the blocks with negative contributions. In this way an optimized LRFEL will have a higher intensity on the optical axis than will a nonoptimized LRFEL. This was demonstrated and quantified from the theory. The full width at half-maximum (FWHM) was numerically calculated from the intensity distribution. It was obtained through the addition of the diffraction produced by each pixel. The FWHM was always near to the one that corresponded to an infinite-resolution lens.

The aim of this paper is to make a rigorous deduction in the scalar Fresnel–diffraction approximation of simple expressions for the light-amplitude distribution, the point-spread function (PSF) and the diffraction efficiency for all the focus. Also the frequency response for monochromatic illumination is analyzed. The characteristics of the optimized LRFEL, which were numerically studied and quantified, are justified from our new analytical expressions. The energy distribution in the focal plane is also studied and evaluated numerically. Several results are appraised in comparison with the nonoptimized case. For each purpose, the theory developed in Ref. 2 is used. In the following section, the basic notation and the two basic expressions that are going to be used are introduced.

2. Theoretical Background

When a single Fresnel lens with focal length f for a wavelength λ is encoded in a pixelated, low-resolution device, with the center-to-center pixel distance given by Δx and Δy, infinite new focal regions appear at the coordinates (kX, lY), where

$$X = \frac{\lambda f}{\Delta x}, \qquad Y = \frac{\lambda f}{\Delta y}, \tag{1}$$

and k and l are arbitrary integers. $X \times Y$ also defines the apparent area of the lens that is associated with each focus.[2] Then, if the device has $P \times Q$ pixels with a rectangular pupil of dimensions $L_x = P\Delta x$ and $L_y = Q\Delta y$, the apparent number of lenses appearing in the device is given by

$$W_x = \frac{L_x}{X}, \qquad W_y = \frac{L_y}{Y}. \tag{2}$$

In Fig. 1(a) a binary LRFEL with $W_x = W_y = 5$ is shown. It resembles an array of 5×5 lenses, but for only one lens was an attempt made to encode.

The light distribution at a (k, l) focus of an infinite phase-stepped LRFEL for plane-wave illumination with a unity amplitude is given by

$$U^{no}_{k,l}(x_i, y_i) = \frac{1}{i\lambda f}\frac{1}{\Delta x \Delta y}\left\{F_{\lambda f}\left[\text{rect}\left(\frac{x}{L_x}, \frac{y}{L_y}\right)\right]\right.$$
$$\left.\times \exp\left[i\frac{2\pi}{\lambda f}(xkX + ylY)\right]\right\} * \text{rect}\left(\frac{x}{\Delta x'}, \frac{y}{\Delta y'}\right), \tag{3}$$

where the asterisk denotes convolution, $F_{\lambda f}$ is the Fourier transform with a λf scale, and no indicates nonoptimized. The first rectangular function defines the rectangular pupil of the device, whereas the second rectangular function defines the pixel of dimensions $\Delta x' \Delta y'$. Other useful parameters are

$$c_x = \frac{\Delta x'}{\Delta x}, \qquad c_y = \frac{\Delta y'}{\Delta y}. \tag{4}$$

To optimize the LRFEL for the $(k = 0, l = 0)$ focus, it was necessary to shift in π the phase of blocks of pixels that contributes with the opposite sign. These blocks have dimensions $(X/c_x, Y/c_y)$. Performing the optimization is equivalent to determining the product of the pupil function with the function $\text{Opt}(x, y)$, the optimizing function, which can be written as

$$\text{Opt}_x(x) = \begin{cases} 1 & 2n\dfrac{X}{c_x} \leq |x| \leq (2n+1)\dfrac{X}{c_x} \\ -1 & (2n+1)\dfrac{X}{c_x} \leq |x| \leq (2n+2)\dfrac{X}{c_x} \end{cases},$$

$$\text{Opt}_y(y) = \begin{cases} 1 & 2m\dfrac{Y}{c_y} \leq |y| \leq (2m+1)\dfrac{Y}{c_y} \\ -1 & (2m+1)\dfrac{Y}{c_y} \leq |y| \leq (2m+2)\dfrac{Y}{c_y} \end{cases},$$

$$\text{Opt}(x, y) = \text{Opt}_x(x)\text{Opt}_y(y), \tag{5}$$

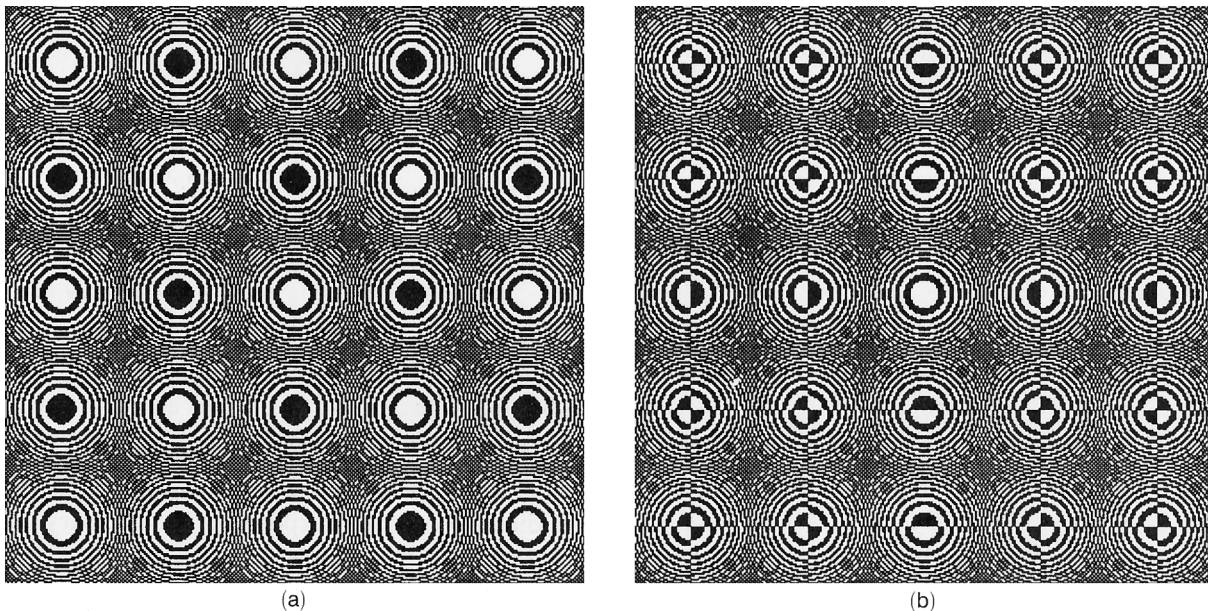where $n, m = 0, 1, 2, 3, \ldots, \infty$. Note that the

(a)

(b)

Fig. 1. Binary LRFEL's: (a) a LRFEL where $W_x = W_y = 5$, and (b) optimized LRFEL where $W_x = W_y = 5$ and $c_x = c_y = 1$.

optimization process affects the lens when $L_x > 2X/c_x$ and $L_y > 2Y/c_y$. Throughout the paper we consider whether these inequalities are verified. In Fig. 1(b) an optimized LRFEL corresponding to Fig. 1(a) for $c_x = c_y = 1$ is shown.

3. Point-Spread Function

A. PSF for the (0, 0) Focus

One can see from Eq. (3) and from taking into account that the pupil function $P(x, y)$ of an optimized LRFEL is

$$P(x, y) = \text{rect}\left(\frac{x}{L_x}, \frac{y}{L_y}\right)\text{Opt}(x, y), \qquad (6)$$

the light-amplitude distribution $U(x_i, y_i)$ of an optimized LRFEL with a focal length f at the (0, 0) focus for plane-wave illumination of wavelength λ is

$$U_{0,0}(x_i, y_i) = \frac{1}{i\lambda f}\frac{1}{\Delta x \Delta y}\, F_{\lambda f}[P(x, y)] * \text{rect}\left(\frac{x}{\Delta x'}, \frac{y}{\Delta y'}\right). \qquad (7)$$

Equation (7) is valid if the following inequality is verified [Eq. (14) of Ref. 2]:

$$\frac{1}{2}\left(\frac{\Delta x'}{\Delta x}\frac{x_i}{X} + \frac{\Delta y'}{\Delta y}\frac{y_i}{Y}\right) \ll 1. \qquad (8)$$

As shown below, the optimization process makes $U_{k,l}(x_i, y_i)$ take negligible values for $|x_i| > 2\Delta x'$ and $|y_i| > 2\Delta y'$; thus, this condition is not a restriction on the calculations in the rest of the paper.

In calculating the Fourier transform of Eq. (7) we consider the case corresponding to the lens constituted by $2N \times 2M$ blocks, for the sake of simplicity. This allows us to write the pupil function $P(x, y)$ as an array of delta functions that have undergone convolution by a rectangular function whose size corresponds to a block. Each delta is affected by the sign of the corresponding block. Thus, we can write

$$P(x, y) = \left(\sum_{n=0}^{N-1}\sum_{m=0}^{M-1}(-1)^{m+n}\left\{\delta\left[x - (2n + 1)\frac{X}{2c_x}\right]\right.\right.$$
$$+ \delta\left[x + (2n + 1)\frac{X}{2c_x}\right]\right\}$$
$$\times \left\{\delta\left[y - (2m + 1)\frac{Y}{2c_y}\right]\right.$$
$$+ \left.\left.\delta\left[y + (2m + 1)\frac{Y}{2c_y}\right]\right\}\right) * \text{rect}\left(\frac{c_x x}{X}, \frac{c_y y}{Y}\right). \qquad (9)$$

By performing the Fourier transform and using the

definitions of our parameters we obtain

$$F_{\lambda f}[P(x, y)] = \sum_{n=0}^{N-1}\sum_{m=0}^{M-1}(-1)^{m+n}\left\{\exp\left[i(2n + 1)\pi\frac{x}{\Delta x'}\right]\right.$$
$$+ \exp\left[-i(2n + 1)\pi\frac{x}{\Delta x'}\right]\right\}$$
$$\times \left\{\exp\left[i(2m + 1)\pi\frac{y}{\Delta y'}\right]\right.$$
$$+ \left.\exp\left[-i(2m + 1)\pi\frac{y}{\Delta y'}\right]\right\}$$
$$\times \frac{XY}{c_x c_y}\,\text{sinc}\left(\frac{x}{\Delta x'}, \frac{y}{\Delta y'}\right). \qquad (10)$$

Performing the addition we obtain

$$F_{\lambda f}[P(x, y)] = \left[4\frac{CS_N\left(N\pi\frac{x}{\Delta x'}\right)CS_M\left(M\pi\frac{y}{\Delta y'}\right)}{\cos\left(\pi\frac{x}{\Delta x'}\right)\cos\left(\pi\frac{y}{\Delta y'}\right)}\right]$$
$$\times \frac{XY}{c_x c_y}\,\text{sinc}\left(\frac{x}{\Delta x'}, \frac{y}{\Delta y'}\right), \qquad (11)$$

where $CS_j(r)$ is

$$CS_j(r) = \begin{cases} \cos^2(r), & j = 1, 3, 5, \ldots, \infty \\ \sin^2(r), & j = 2, 4, 6, \ldots, \infty \end{cases}, \qquad (12)$$

In Eq. (11) the sinc function modulates an oscillatory function. Using Eq. (11) in Eq. (7) and defining the adimensional coordinates as

$$s = \frac{x}{\Delta x'}, \qquad t = \frac{y}{\Delta y'},$$
$$s_i = \frac{x_i}{\Delta x'}, \qquad t_i = \frac{y_i}{\Delta y'}, \qquad (13)$$

we finally obtain

$$U_{0,0}(s_i, t_i) = \frac{4\lambda f}{i\Delta x \Delta y}\int_{-1/2+s_i}^{1/2+s_i}\frac{CS_N(N\pi s)}{\cos(\pi s)}\,\text{sinc}(s)\text{d}s$$
$$\times \int_{-1/2+t_i}^{1/2+t_i}\frac{CS_M(M\pi t)}{\cos(\pi t)}\,\text{sinc}(t)\text{d}t, \qquad (14)$$

where the convolution is explicitly done. From Eqs. (13) and (14), $\Delta x'$ and $\Delta y'$ act as scale factors on the PSF. The resulting integrals can easily be evaluated with standard numerical techniques.[4] The main characteristics of the resultant expression can now be studied. For this purpose, it is necessary only to study one of the integrals.

In Fig. 2 the integrand of the first integral of Eq. (14) for $N = 11$ is represented, along with the modulating sinc function. The integrand has an
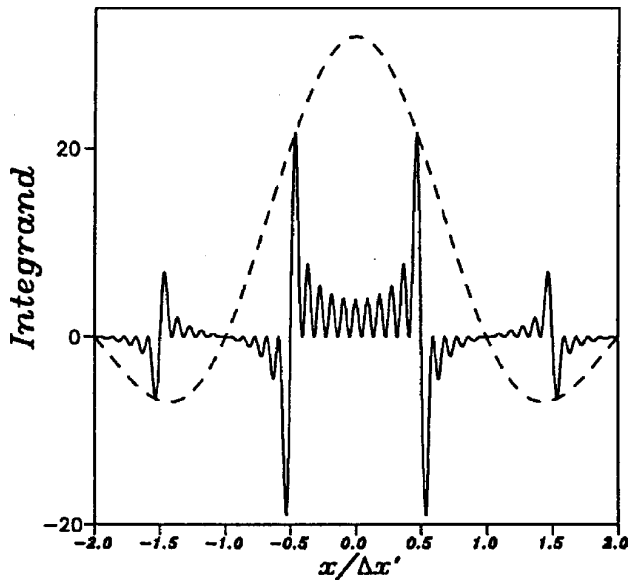
Fig. 2. Integrand of Eq. (14) for $N = 11$ (Solid curve). The integrand has absolute maxima and minima for $|s| \approx \pm0.5$. The modulating sinc function is also shown (dashed curve). The y axis is in arbitrary units.

absolute maximum and a minimum at $|s| \approx \pm0.5$ because of the cosine function in the denominator. As N increases, the maximum (minimum) value increases (decreases), and more oscillations take high values near the maximum (minimum). For $s_i = 0$, the integration interval is $(-0.5, 0.5)$, and the integrand is always positive. Thus, the intensity $|U(0, 0)|^2$ increases with N as expected. It should be noted that the distance between the zeros of the integrand is just $1/N$, so if s_i is incremented in $1/N$ an absolute maximum goes out of the integration interval and an absolute minimum is now included. This produces a high decrease in the value of $U(s_i, t_i)$. From this fact it can be concluded that the FWHM is approximately $\text{FWHM} \approx \Delta x'/N$, i.e., almost double the FWHM value corresponding to the infinite-resolution case. The FWHM was numerically calculated in Ref. 2, and this fact was observed and quantified. Thus, optimization allows us to obtain a higher and a thinner PSF than does the nonoptimized lens. This is illustrated in Figs. 3, where the PSF is computed from Eq. (14) for several cases: Figs. 3(a), 3(b), 3(d), and 3(f) correspond to the PSF of nonoptimized LRFEL's that comprise 2 × 2 block, 4 × 4 block, 6 × 6 block, and, as a limit case, 22 × 22 block lenses; Figs. 3(c), 3(e), and 3(g) correspond to the PSF's of optimized LRFEL's for the same block lenses, respectively, excluding the limiting case. Note from Eq. (5) that a 2 × 2 block lens has no phase shifts and that the optimized lens coincides with the nonoptimized lens.

B. PSF for a (k, l) Focus

Following the same steps as in the Subsection 3.A. but taking as the starting point the amplitude-distribution expression given in Eq. (3), with k and l

being different from zero, we obtain for the amplitude distribution for a (k, l) focus the following expression:

$$U_{k,l}(s_i, t_i) = \frac{4\lambda f}{i\Delta x \Delta y} \int_{-1/2+s_i}^{1/2+s_i} \left[\frac{CS_N(N\pi s)}{\cos(\pi s)} \, \text{sinc}(s) \right]$$

$$\times \exp(i2\pi k c_x s) ds$$

$$\times \int_{-1/2+t_i}^{1/2+t_i} \left[\frac{CS_M(M\pi t)}{\cos(\pi t)} \, \text{sinc}(t) \right]$$

$$\times \exp(i2\pi l c_y t) dt. \qquad (15)$$

This expression is explicitly dependent on c_x and c_y. Now a linear phase variation affects the integrand and highly modifies the PSF. A particular case of special interest is $c_x = c_y = 1$. The shape of the lens for this case is as the same as the one shown in Fig. 1(b). Lenses with this shape are listed in the bibliography for studies of image derivation and alignment.[5–7] To justify the shape of the PSF for this particular case (i.e., $c_x = c_y = 1$), the real and imaginary parts of the first integral for $k > 0$ should be studied in terms of the behavior of factors affecting the complex exponential (the terms between square brackets) and the symmetry and antisymmetry of the real and imaginary parts of the integrals involved.

Because of structures of the factors (represented in Fig. 2), the real part of the integrand will take only important values for $s_i = 0$. For this value, the real part is symmetric. For small values of N the factors have a smooth variation with s and the value of the real part of the integral is small. (If they are constant the integral is zero.) If we consider N to increase, the factors have a higher variation, especially for $s \to 0.5$. Then the value at the origin increases with N. Conversely, if we consider higher values of k for a constant N, the frequency of the oscillations of the integrands increases making the value of the integral tend to zero. If a little variation of s_i around zero is considered, a big lobe with an opposite contribution is included and a contributing lobe is excluded, thus making the real part of the integral tend to zero. Thus, the real part takes a maximum for $s_i = 0$ and has a width of $1/N$, approximately. Also because of the symmetry of the integrand, the imaginary part is null for this value of s_i. But for $s_i = 0.5$ the range of integration is $(0, 1)$ and the factors are approximately antisymmetric respect to $s = 0.5$. Following analogous reasonings, we can deduce that an important maxima that is due to the imaginary part of the integral occurs around this point. The width of this maxima is larger because of the fact that, for small variations of s_i, no important lobes are included in or excluded from the integration interval; this happens for an increment of s_i of approximately ±0.5. For $s_i = -0.5$ we have another maxima with the opposite sign. Because of the sinc function of the factors, the integral does not have another important maximum. Thus, in general, the representation of the integral leads to a

Fig. 3. Three-dimensional representation of the PSF corresponding to the $(0, 0)$ focus of a LRFEL constituted by $2N \times 2N$ blocks. The drawing has an area of 2×2 pixels: for (a) $N = 1$ (optimized and nonoptimized lenses coincide), (b) nonoptimized $N = 2$, (c) optimized $N = 2$, (d) nonoptimized $N = 3$, (e) optimized $N = 3$, (f) nonoptimized $N = 11$, and (g) optimized $N = 11$.
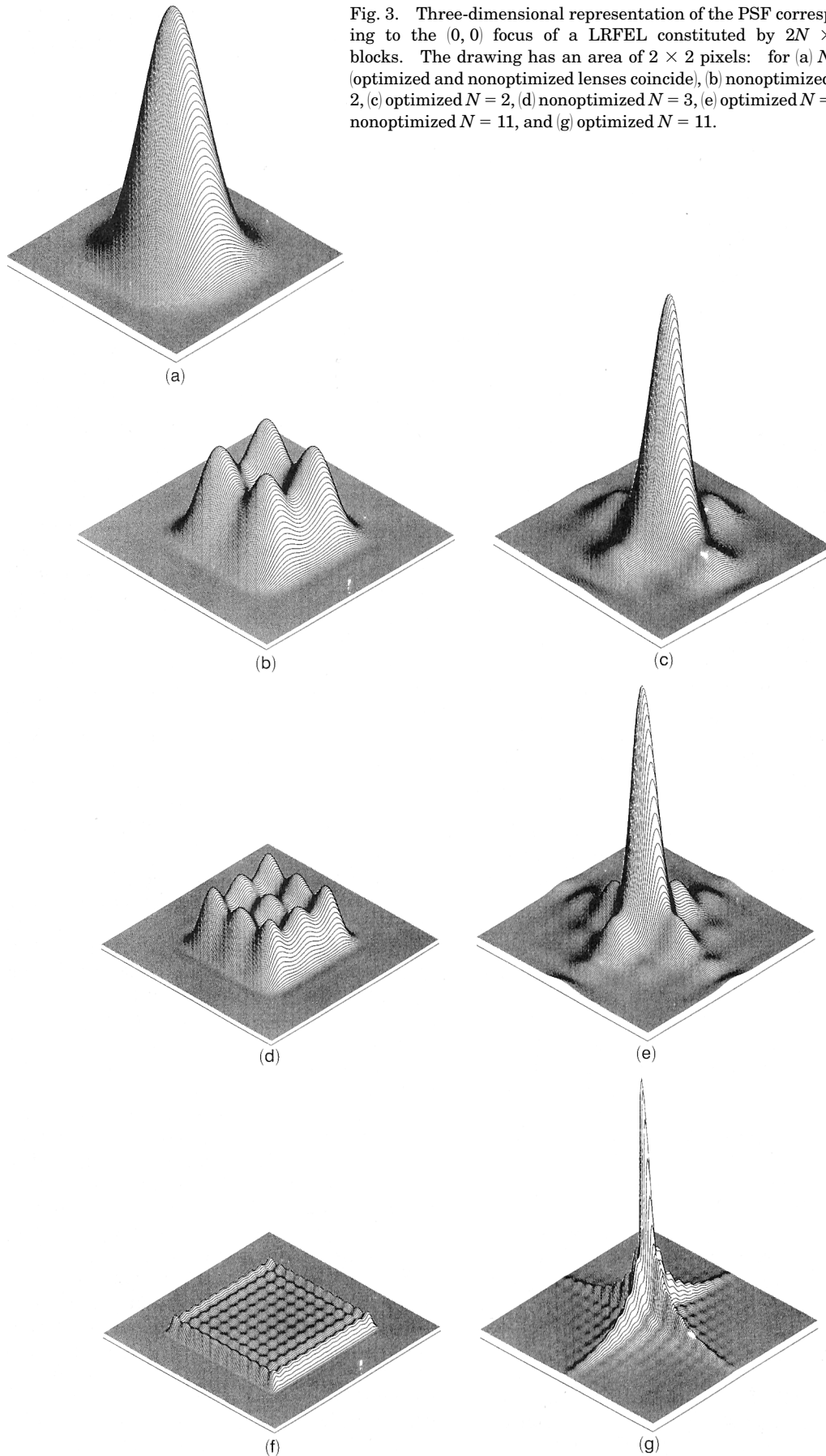
figure composed of two lobes with opposite signs that are centered at $s_i \approx \pm 0.5$, with an approximate unity width and separated by a maximum with $1/N$ width. As an illustration of this description, Figs. 4 show the square modulus of Eq. (14) (the PSF) for an optimized lens with $N = 3$ with $(k, l) = (1, 0), (2, 0), (1, 1), (2, 2)$. The amplitudes of the lobes have opposite signs in such a way that the $(-1, 0)$ can perform a derivative in the x direction and $(-1, -1)$ makes the $\delta^2/\delta x \delta y$ (Ref. 5).

4. Diffraction Efficiency

To calculate the energy concentrated in a (k, l) focus, $E_{k,l}$, the following integral must be evaluated:

$$E_{k,l} = \int_{-\infty}^{\infty} \int_{-\infty}^{\infty} |U_{k,l}(x, y)|^2 \mathrm{d}x \mathrm{d}y. \tag{16}$$

The direct calculation of Eq. (16) is rather difficult. To simplify the calculations, the Parseval theorem can be used.[8] This theorem establishes the possibility of one's evaluating $E_{k,l}$ by one's performing the integral on the square modulus of the Fourier transform of $U_{k,l}$. Applying the Parseval theorem we obtain

$$E_{k,l} = [\lambda f c_x c_y]^2 \int_{-\infty}^{\infty} \int_{-\infty}^{\infty} \mathrm{rect}^2 \left[\left(f_x - \frac{k}{\Delta x} \right) \frac{\lambda f}{L_x}, \left(f_y - \frac{l}{\Delta y} \right) \frac{\lambda f}{L_y} \right]$$

$$\times \left| \mathrm{Opt} \left[\lambda f \left(f_x - \frac{k}{\Delta x} \right), \lambda f \left(f_y - \frac{l}{\Delta y} \right) \right] \right|^2$$

$$\times \mathrm{sinc}^2 (\Delta x' f_x, \Delta y' f_y) \mathrm{d}f_x \mathrm{d}f_y, \tag{17}$$

where f_x and f_y are the frequency coordinates in the Fourier space. This is the volume under the product of a squared sinc function and the rectangular function. Note that $|\mathrm{Opt}(x, y)|^2 = 1$ for all x and y, hence the optimization process has no effect on the diffraction efficiency. The only effect of the optimization process is to change the energy distribution. It can also be deduced from Eq. (17) that an alternative definition of $\mathrm{Opt}(x, y)$ makes the efficiency equal or lower. This result is because the maximum value of the amplitude of $\mathrm{Opt}(x, y)$ is, of course, unity. Thus, each (k, l) focus of the optimized LRFEL has the same diffraction efficiency as the (k, l) focus of the nonoptimized LRFEL. The diffraction efficiency of the LRFEL has been analytically calculated in Ref. 9.

5. Energy Distribution

As we are interested in the energy distribution in the focal region for the optimized focus $(k = 0, l = 0)$, we have numerically studied the cases corresponding to Figs. 3. The results are shown in Figs. 5, in which the amount of energy concentrated in the rectangular region defined by $[(-x/\Delta x', x/\Delta x'), (-y/\Delta y', y/\Delta y')]$ is represented. In these figures the energy distribution of the nonoptimized LRFEL is also represented. Curiously, for the optimized lenses, the energy distribution is quite independent of N, and 50% of the energy is always concentrated in an area approximately defined by $|x/\Delta x'|, |y/\Delta y'| \leq 0.2$. Thus, the energy distribution is optimized, but it is not comparable with the infinite-resolution case.
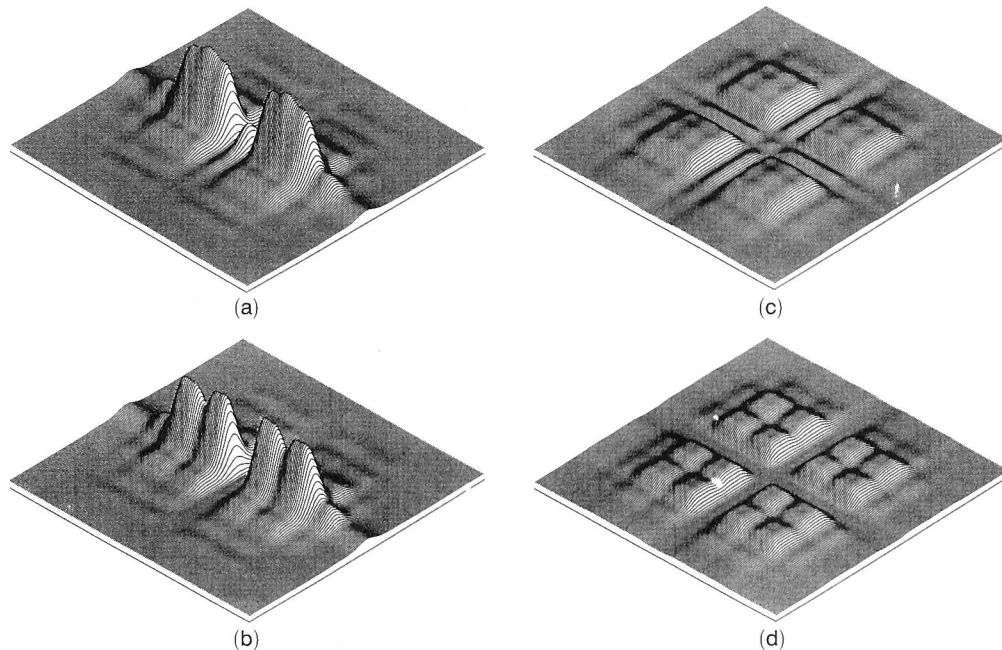

(a)

(b)

(c)

(d)

Fig. 4. Three-dimensional representation of the PSF of an optimized LRFEL with 6×6 blocks in an area of 3×3 pixels [the scale of the figures is the same as that of Fig. 3(c) and 3(d): for (a) $k = 0$ and $l = 1$, (b) $k = 0$ and $l = 2$, (c) $k = 1$ and $l = 1$, and (d) $k = 2$ and $l = 2$.

6. Frequency Analysis of the Optimized LRFEL for Monochromatic Illumination

A. Frequency Analysis for the (0, 0) Focus

To obtain the coherent transfer function H, the Fourier transform of the amplitude distribution given in Eq. (7) must be performed.[8] Taking $1/\Delta x$ and $1/\Delta y$ as natural-frequency unities and defining as follows the adimensional frequency coordinates:

$$u = \Delta x f_x, \qquad v = \Delta y f_y, \tag{18}$$

where f_x and f_y are the frequency coordinates in the Fourier space, we obtain for $H(u, v)$

$$H(u, v) = \lambda f c_x c_y \, \text{rect}\!\left(\frac{u}{W_x}, \frac{v}{W_y}\right)$$
$$\times \text{Opt}(Xu, Yv)\text{sinc}(c_x u, c_y v). \tag{19}$$

Using the definition of Opt [Eq. (5)] we get

$$H(u, v) = \lambda f c_x c_y \, \text{rect}\!\left(\frac{u}{W_x}, \frac{v}{W_y}\right) |\text{sinc}(c_x u, c_y v)|. \tag{20}$$

Thus, as a result of the optimization process, the transfer function always becomes positive. If
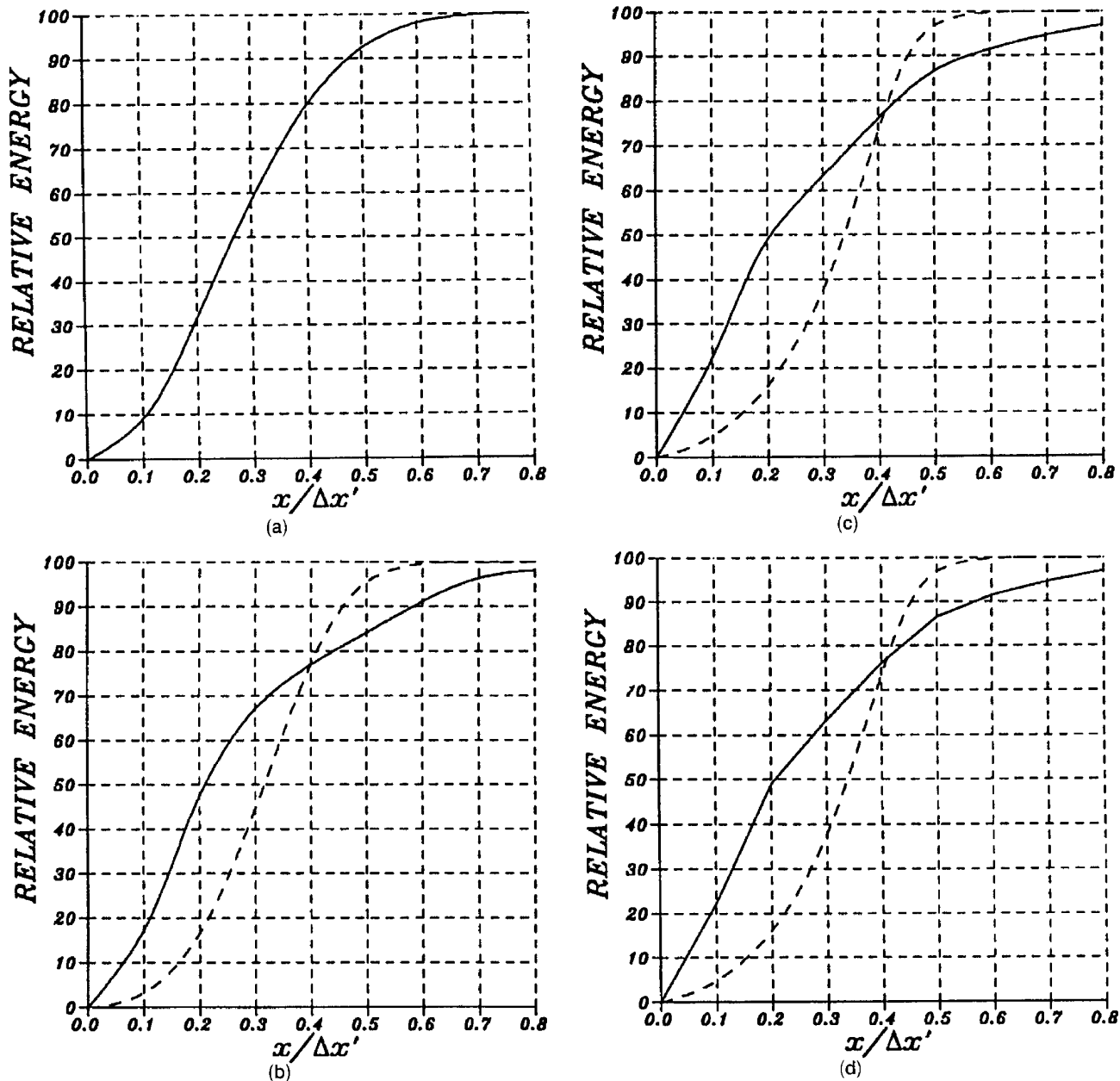

Fig. 5.   Energy distribution for the $(k = 0, l = 0)$ focus for an optimized (solid curve) and a nonoptimized LRFEL (dashed curve) composed of $2N \times 2M$ blocks: for (a) $N = 1$ (optimized and nonoptimized lenses coincide), (b) $N = 2$, (c) $N = 3$, and (d) $N = 11$.
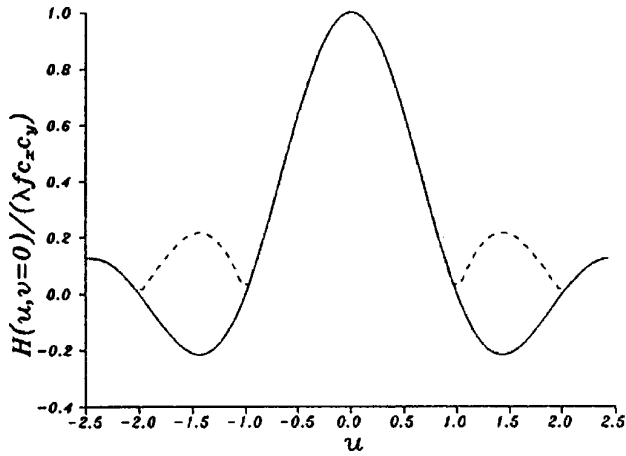
Fig. 6. Comparison of a section of the coherent transfer function H for an optimized (dashed curve) and a nonoptimized (solid curve) LRFEL for $k = l = 0$, $c_x = c_y = 1$, and $W_x = W_y = 5$.

Fig. 7. Coherent transfer function H for an optimized LRFEL for $k = 1$, $l = 0$, $c_x = c_y = 1$, and $W_x = W_y = 5$.

Opt$(x, y) = 1$ (i.e., we have a nonoptimized LRFEL), then the sinc function can cause negative values for a certain range of frequencies. This is illustrated in Fig. 6 for $c_x = c_y = 1$ and $W_x = W_y = 5$. Negative values of H imply an inversion of contrast.[8] Thus, clearly, the coherent transfer function of an optimized LRFEL is the optimum one. Note that the cut-off frequency depends on the dimensions of the pupil and is given by $(u = W_x/2, v = W_y/2)$ and the first zero is determined by $(u = 1/c_x, v = 1/c_y)$. Analog comments apply for the incoherent optical transfer function (OTF), which is obtained from the normalized autocorrelation of the coherent transfer function. The OTF for the nonoptimized lens will have oscillations with periodical changes of sign. The OTF for the optimized lens is always positive, and the cut-off frequency is exactly double and also the first zero.

B. Frequency Analysis for the (k, l) Focus

Performing the Fourier transform of Eq. (3) [but taking as the pupil function Eq. (6)] and following the same steps as in Section 6.A., we obtain for the (k, l) focus the following coherent transfer function:

$$H_{k,l}(u, v) = \lambda f c_x c_y \, \mathrm{rect}\left[\frac{(u - k)}{W_x}, \frac{(v - l)}{W_y}\right]$$
$$\times \mathrm{Opt}[X(u - k), Y(v - l)]\mathrm{sinc}(c_x u, c_y v).$$
$$(21)$$

The case of $c_x = c_y = 1$ is now considered. This case is represented in Fig. 7 for $k = 1$, $l = 0$, $c_x = c_y = 1$, and $W_x = W_y = 5$. The two halves of the main lobe of the sinc function always have opposite signs. This implies a derivative effect in the coherent image-formation process. The signs of the other small lobes depend on k and l; the Opt function causes a correct change of sign (for derivation purposes) for the frequency range $[(-\infty, k/c_x), (-\infty, l/c_y)]$ for k,
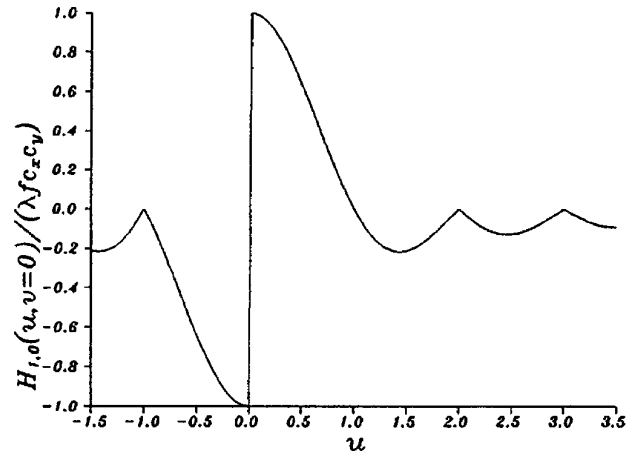
$l > 0$ and $[(k/c_x, \infty), (l/c_y, \infty)]$ for k, $l < 0$. Other frequencies have a wrong sign, but note that H takes small values for those frequencies and that the error is smaller for increasing k and l [the only purpose for the optimization process was to improve the PSF of the $(0, 0)$ focus]. Note that the rectangular function is shifted for each (k, l) focus but that the main lobe is always included for the encoded orders $(|k| < W_x/2, |l| < W_y/2)$. The OTF clearly does not preserve these properties and has no interesting characteristics.

7. Conclusions

To improve the performance of the $(k = 0, l = 0)$ focus of the LRFEL so that it might be used as a single lens when a short focal length is encoded, Carcolé et al.[2] designed an optimization process. From the resultant expressions, the following main characteristics of the PSF have been deduced in this paper:

(1) For the $(0, 0)$ focus the FWHM is almost double that of a lens of infinite resolution (diffraction limited). The spatial resolution is thus much better than the nonoptimized lens; it has a FWHM equal to the size of the pixel for a short-focal-length encoded lens. The intensity in the optical axis increases with the number of blocks encoded.
(2) At the (k, l) focus the PSF has a special interest for c_x, $c_y = 1$. At these focuses, derivatives of the image are obtained.
(3) The diffraction efficiency for all focuses coincides with the nonoptimized case, and it has been demonstrated that it is impossible to increase the diffraction efficiency.
(4) The energy distribution for the $k = l = 0$ focus is better than for the nonoptimized case, but it is not comparable with the infinite-resolution case. Approximately 50% of energy is concentrated in a region defined by $|x| < 0.2\Delta x'$, $|y| < 0.2\Delta y'$. The energy distribution is to a very small degree dependent on the number of encoded blocks.

(5) The frequency analysis shows an optimum performance for the optimized lenses for the $(0, 0)$ focus. The coherent transfer function and the OTF for the nonoptimized lens have periodical changes of sign, but for the optimized lens the signs are always positive.

(6) For any (k, l) focus other than $k, l = 0$, with $k < W_x/2$, $l < W_y/2$ and $c_x = c_y = 1$, its ability to perform derivatives has also been shown at least for the frequency range $(-1/\Delta x, 1/\Delta x)$ to $(-1/\Delta y, 1/\Delta y)$, which corresponds to the main values of the coherent transfer function.

Finally, an optimized LRFEL produces a better imaging quality than does a nonoptimized LRFEL for the $(k = 0, l = 0)$ focus. For the particular case of $c_x = c_y = 1$ and coherent illumination, the other focus gives derivatives of the image. Thus, a further study of the possible application of this type of lens in optical-image processing is necessary.

References

1. E. C. Tam, S. Zhou, and M. R. Feldman, "Spatial-light-modulator-based electro-optical imaging system," Appl. Opt. **31,** 578–580 (1992).
2. E. Carcolé, J. Campos, and S. Bosch, "Diffraction theory of Fresnel lenses encoded in low-resolution devices," Appl. Opt. **33,** 162–174 (1994).
3. D. M. Cottrell, J. A. Davis, T. Hedman, and R. A. Lilly, "Multiple-imaging phase-encoded optical elements written as programmable spatial light modulators," Appl. Opt. **29,** 2505–2509 (1990).
4. W. H. Press, B. P. Flannery, S. A. Teukolsky, and W. T. Vetterling, *Numerical Recipes in C* (Cambridge U. Press, Cambridge, 1988).
5. J. A. Davis, W. V. Brandt, D. M. Cottrell, and M. Bunch, "Spatial image differentation using programmable binary optical elements," Appl. Opt. **30,** 4610–4614 (1991).
6. S. B. Viñas, Z. Jaroszewicz, A. Kolodziejczyk, and M. Sypek, "Zone plates with black focal spots," Appl. Opt. **31,** 192–198 (1992).
7. J. Ojeda-Castañeda, P. Andrés, and M. Martínez-Corral, "Zero axial irradiance by annular screens with angular variation," Appl. Opt. **31,** 4600–4602 (1992).
8. J. W. Goodman, *Introduction to Fourier Optics* (McGraw-Hill, New York, 1968).
9. E. Carcolé, J. Campos, I. Juvells, and S. Bosch, "Diffraction efficiency of low-resolution Fresnel encoded lenses," Appl. Opt. **33,** 6741–6746 (1994).